ISSN: 2633-4828 Vol. 4 No.1, June, 2022

International Journal of Applied Engineering & Technology

DIELECTRIC AND MAGNETIC STUDIES OF MIXED FERRITES USING CITRIC ACID ASSISTED WET-CHEMICAL METHOD

Syeda Ayesha[1], Suresha M Shivalingaiah[2], M Harish Kumar[3*] and Shilpa S[4]

[1]Department of Chemistry, Government First Grade College, Kuvempunagar, Mysuru-570023, Karnataka, India

[2]Department of Chemistry, Government Engineering College, Kushalnagar-571234, Madikeri, Karnataka

[3]Department of Physics, Government Engineering College, Bedarapura, Chamrajanagar-571313

[4]Department of Physics, Government First Grade College, Kadugudi, Bengaluru-560067, Karnataka

*harishkagalipur@gmail.com

ABSTRACT

Using wet chemical method preferably auto-combustion approach, nickel ferrite nanoparticles doped with Cu^{+2} with the basic chemical composition $Cu_xNi_{1-x}Fe_2O_4$ (x=0.0 to 1.0 in steps of 0.25) were prepared. Phase confirmation of the proposed samples was confirmed through XRD studies. XRD pattern of the prepared ferrites revealed single phase spinel cubic structure. At room temperature, using HIOKI LCR meter (Model no: 3520-50) the dielectric measurements in the frequency range 10^2 Hz to 10^6 Hz were performed. Dielectric constant (ε') and dielectric loss tangent (tan δ) of synthesized nano-materials were investigated as a function of frequency and Cu^{+2} concentration and all the samples exhibited dielectric dispersion. Magnetic measurements for $Cu_xNi_{1-x}Fe_2O_4$ nano-ferrites were carried out at room temperature using a vibrating sample magnetometer (VSM), and all the samples of the system $NiCuFe_2O_4$ exhibited ferri-magnetic behavior.

Keywords: Wet-chemical; Precursors; Dielectric constant; VSM.

1. INTRODUCTION

Soft spinel ferrites with nano-structures are of great interest due to their potential use in diverse fields and these ferrites have excellent physio-chemical properties such as , low toxicity, highly tunable properties, like its dielectric, magnetic properties, which can be easily modified just adopting various synthesis techniques, synthesis environments and other factors such as the type of organic fuel used for the synthesis, P_H of the redox solution, composition of the divalent or trivalent metal ions in respective tetrahedral or octahedral sites, types of additives and sintering temperature and sintering duration etc [1-3]. Nano-structured magnetic oxides are currently considered among the widely successful magnetic nanoparticles (MNPs) that can be extensively used for various technological and in medical applications such as in various sensor applications, in storage medium applications, contrast enhancement in magnetic resonance imaging, in auto-mobile industry suspension systems using magnetic fluids, targeted drug delivery and in many more technological devices and applications. [4-5].

Spinel magnetic oxide materials consists of Fe_2O_3 as one of the integral part and have spinel ($MO.Fe_2O_3$) cubic structure, here M is a divalent metal ion(s) such as Co^{+2}, Zn^{+2}, Mg^{+2}, Ni^{+2}, Cd^{+2}, Cu^{+2} or a combination of these ions. These samples, which are ferri-magnetic in nature when exposed to external applied magnetic field, exhibit magnetic hysteresis (M-H curve) and at the same time exhibit spontaneous magnetization. Various properties of these ferrites with MFe_2O_4 structure is because of distribution of divalent and trivalent metal ions among the two interstitial voids such as tetrahedral (A) and octahedral (B) sites [5].

In case of inverse spinel structure half of the trivalent metal ions occupy tetrahedral (A-sites) and half in octahedral (B-sites), the remaining cations being randomly distributed among the B-sites. Inverse spinel ferrites are represented by the formula $(Me^{+3})_A [M^{+2}Me^{+3}]_B O_4$. Nickel ferrite belongs to inverse spinel with Ni^{+2} at octahedral (B-site) and Fe^{+3} ions distributed equally in both, tetrahedral (A-site) and octahedral sites (B-site). Nickel ferrites are used in numerous electronic device applications because of their high permeability, high electrical resistivity, mechanical hardness, and chemical stability [6-11].

$CuFe_2O_4$ is also a very interesting inverse spinel ferrite material due to its excellent magnetic properties together with electrical and semiconducting properties [12]. Moreover copper ferrite exhibits a phase transition at different

temperatures due to John-Teller (J-T) distortion of Cu^{+2} ions [13]. $CuFe_2O_4$ exhibits p-type semiconducting behavior possessing a band gap of 1.39 eV. $CuFe_2O_4$ exists in the tetragonal phase at low temperatures having c/a= 1.059 and at high temperatures exists in cubic phase with a = 8.379Å [14]. J-T effect is a prominent factor for the reduction of crystal symmetry causing a phase transition from cubic to tetragonal phase. $CuFe_2O_4$ is an inverse spinel structure with the formula unit $(Fe^{3+})[Cu^{2+}Fe^{3+}]O_4^{-2}$ and its theoretical lattice parameter is 8.365 Å.

In our present study, when divalent metal ions such as Cu^{+2} is substituted in nickel ferrite, they form the technologically important materials which are used in functional devices such as in field sensors, heterogeneous catalysis, and in various sensors. Here, using wet chemical method preferably auto-combustion approach, nickel ferrite nanoparticles doped with Cu^{+2} with the basic chemical composition $Cu_xNi_{1-x}Fe_2O_4$ (x=0 to 1: in steps of 0.25) were prepared using nitrate-citrate auto-combustion method. This method is a self-propagating thermally-induced reaction of a gel, obtained from aqueous solutions containing metallic nitrates which acts as oxidizer and an organic fuel. Stoichiometric proportions between fuel and metallic nitrates are calculated according to the valencies of the reacting elements so as to provide the relation of oxidizer/fuel equal to one [12]. Here, metallic nitrates are preferred as starting materials which are also known as precursors, because of their water-soluble nature, have low ignition temperatures and are easy to prepare.

2. MATERIALS AND METHODS

Nano-powders of mixed ferrite of the system $Cu_xNi_{1-x}Fe_2O_4$, here (x = 0.0, 0.25, 0.5, 0.75 and 1.0) were prepared using auto-combustion method. Precursors for starting the materials synthesis are Nickel Nitrate hexa-hydrate ($Ni(NO_3)_2.6H_2O$), Ferric Nitrate nonahydrate ($Fe(NO_3)_2.9H_2O$), Copper Nitrate tri-hydrate ($Cu(NO_3)_2.3H_2O$ and Citric acid monohydrate ($C_6H_8O_7.H_2O$), all chemicals are of analytical reagent-AR grade with purity more than 99%. Aqueous solutions of metallic nitrates and Citric acid, which is here taken as organic fuel needed for auto-combustion reaction and are taken as per the stoichiometry. Equi-molar citric acid was added into the aqueous solution of metallic nitrates. Aqueous solution containing redox mixture was taken in a silica crucible and is allowed in to a muffle furnace, which was already pre-heated to a temperature of 550^0C. Redox mixture finally yields porous and fluffy voluminous ferrite powder. Obtained fluffy material was ground to get ferrite powders. As-burnt ash was sintered at 950^0C for 5 hours to get better crystallization and homogeneous cation distribution in the proposed spinel and finally ground to get proposed ferrite nano-powders.

$Cu(NO_3)_2.3H_2O + Ni(NO_3)_2.6H_2O + Fe(NO_3)_3.9H_2O + C_6H_8O_7.H_2O \rightarrow NiCuFe_2O_4 + CO_2\uparrow + N_2\uparrow +$ Gaseous Products.

Phase confirmation of the proposed samples were investigated using X-ray diffraction (XRD) studies using Bruker AXS D8 Advance X-ray diffractometer (Cu-K_α radiation, λ=1.5406 Å), a working voltage of 40kV at 40mA of current. Diffraction data were collected in the 2θ range $10\text{-}80^0$. Morphology of the sintered samples has been investigated using Field Emission Scanning Electron Microscope (JEOL Model 7610FPLUS). Parallel capacitance, C_p and dissipation factor, tanδ as a function of frequency in the range 20 Hz-5 MHz were measured using a precision LCR meter. Real and imaginary parts of dielectric permittivity (ε') and (ε") were computed using the formulae [13],

$$\varepsilon' = Ct/\varepsilon_0 A \quad (1)$$

$$\varepsilon'' = \varepsilon' \tan\delta \quad (2)$$

Where, t is the thickness and A, the area of the pellet.

The ac conductivity, σ_{ac} was determined from the dielectric loss factor using a relation

$$\sigma_{ac} = \omega \varepsilon_0 \varepsilon'' \quad (3)$$

Where, ε_0 is the vacuum permittivity and $\omega = 2\pi f$ with f being frequency.

3. RESULTS AND DISCUSSION

3.1 Phase and Surface Morphology

PXRD diffractograms of the samples of the mixed ferrite system with chemical composition $Cu_xNi_{1-x}Fe_2O_4$ (here x= 0.0 to 1.0 in steps of 0.25) are presented in Figure 1. Presence of (220), (311), (400), (422), (511), (440) and (533) planes indexed for the cubic phase of spinel ferrites. Here, in the obtained XRD spectrum, highest intensity peak at $2\theta = 35^0$confirms the formation of the mixed ferrite system.

For $NiFe_2O_4$, JCPDS Card No: 10-0325 and JCPDS Card No: 77-0010 for $Ni_{0.5}Cu_{0.5}Fe_2O_4$ and for $CuFe_2O_4$, JCPDS Card No: 34-0425. Synthesized nano-samples of mixed ferrite were labeled as NFO, NCu-1, NCu-2, NCu-3 and CuFO for the $NiFe_2O_4$, $Ni_{0.75}Cu_{0.25}Fe_2O_4$, $Ni_{0.5}Cu_{0.5}Fe_2O_4$, $Ni_{0.25}Cu_{0.75}Fe_2O_4$ and $CuFe_2O_4$. Here ionic radii of Ni^{+2} is 0.69 Å, whereas for Cu^{+2} it is 0.71 Å. Peaks in XRD spectrum slightly shifts towards the right side from the origin, this can be easily understood from Shannon's radii of the constituent ions as the smaller Ni^{+2} ions with the ionic radii (0.69Å) are replacing the larger radius Cu^{+2} ions with ionic radii (0.71 Å). This substitution of metallic ion of larger ionic radii (Cu^{+2}) not only alters lattice parameter buy also its magnetic properties.

Microstructures were studied by placing the samples under Scanning electron microscope. Micrographs of the sintered samples are depicted in Fig. 2 (a-c), shows the surface structure for the proposed samples. All the samples are having well dispersed and dense structure.

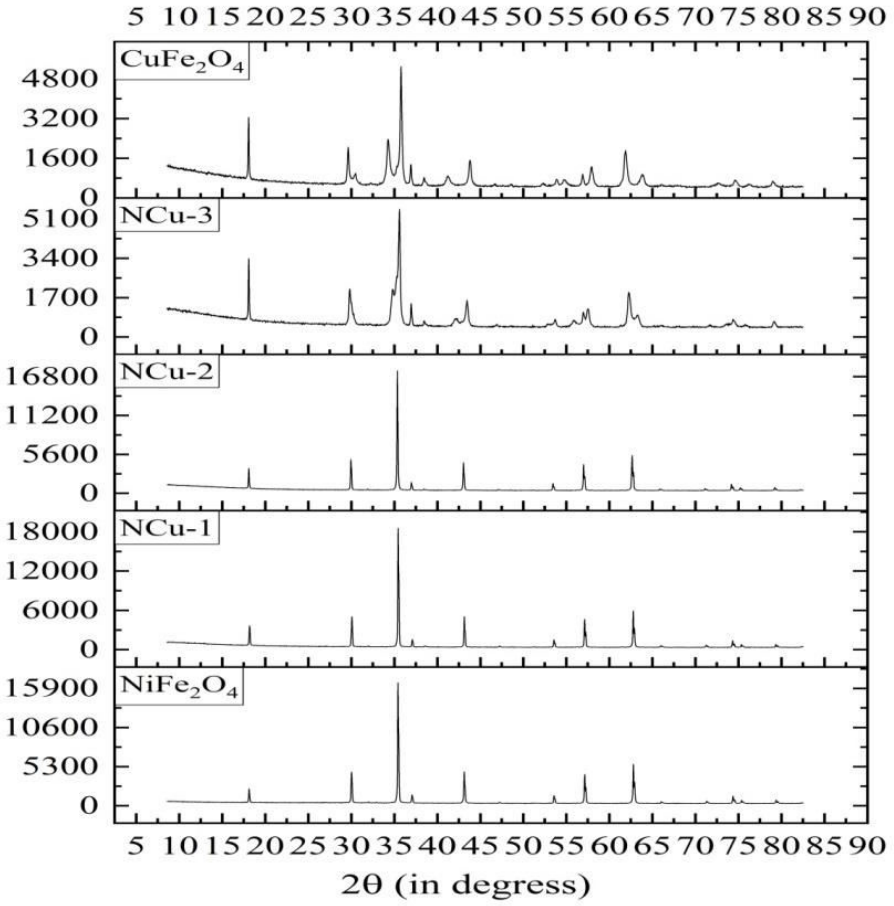

Fig.1: XRD Spectrum of Pure NFO ,CuFO, NCu-1, NCu-2 and NCu-3 samples

FESEM Surface Morphology Studies

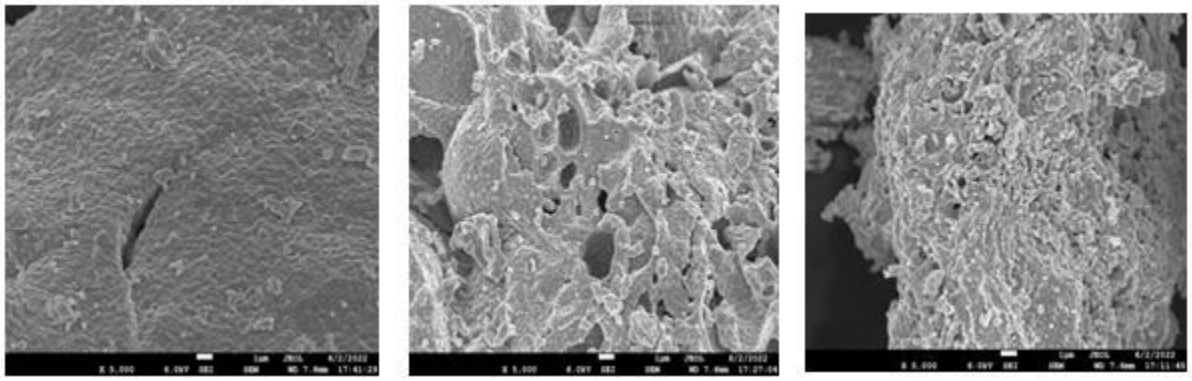

Fig. 2 Micrographs of (a) $Ni_{0.75}Cu_{0.25}Fe_2O_4$ (b) $Ni_{0.5}Cu_{0.5}Fe_2O_4$ (c) $Ni_{0.25}Cu_{0.75}Fe_2O_4$

3.2 Dielectric Studies

Dielectric parameters such as permittivity, ε' and ac conductivity (σ_{ac}) with respect to variation in frequency at room temperature for the synthesized samples is shown in Fig.3. From the Fig.3 (a), it is clear that ε' decreases with increasing frequencies and remains almost independent at higher frequencies. Variation of dielectric constant with applied frequency is due to charge transport relaxation. Dielectric dispersion is common in ceramics like ferrites and is attributed to Maxwell and Wagner type of interfacial polarization [14-16], as the dielectric constant is a combined effect of dipolar, electronic, ionic and interfacial polarizations. Since ionic polarization decreases with frequency, at higher frequency cycle rates, the constituent electric dipoles are unable to follow the quick variations of the alternating applied electric field and hence, measured ε' also decreased with frequency. Larger values of permittivity are related with space charge polarization at grain boundary and heterogeneous dielectric structure.

By electron exchange between Fe^{+2} and Fe^{+3}, displacement of electrons takes place with the applied field and these electrons determine polarization. Polarization decreases with increase in frequency and for further increase, the electric exchange between Fe^{+2}/Fe^{+3} cannot follow the alternating field hence reaches the constant value [17].

Variation in the dielectric loss for all the proposed series of samples upto the frequency range of 1 MHz at room temperature is shown in Fig. 3(c). Values of loss tangent (tanδ) represent the attenuation in these proposed ceramics and polarization being unable to respond to applied external frequency. Similar nature of curves for both ε' and tanδ are almost similar and may be correlated to the domain wall motion with the applied field, the electron exchange between Fe^{+2} and Fe^{+3} ions can correlate with the dielectric properties exhibited by proposed samples.

In order to understand the type of charge carriers and type of polarons responsible for conduction, ac conductivity, σ_{ac} were estimated as per $\sigma_{ac}= \omega \varepsilon_0 \varepsilon''$, with ε_0 is the permittivity of free space and $\omega=2\pi f$.

For the synthesized samples, variation of a.c conductivity, σ_{ac} with frequency, ln (ω), is shown in Fig.3 (d). Obtained plots are almost linear for the entire range of frequency except at lower frequencies. Linear variation of σ_{ac} with frequency confirms that, conduction in mixed spinel ferrite occurs by the hopping of charge carriers between the localized states which confirms the small polaron type of conduction [18]. Conduction mechanism in spinel ferrites can be explained based on the hopping of charge carriers between Fe^{+2} and Fe^{+3} ions on octahedral lattice sites. Increase in the frequency of the applied field accelerates the hopping of charge carriers thereby enhancing the overall conduction process, thereby increasing the conductivity. At higher frequencies, ac conductivity (σ_{ac}), remains constant because the hopping frequency of the charge carriers no longer follows the external applied field variations and lags behind it. However, the decrease in conductivity values at lower frequencies can be correlated to conduction by mixed polarons.

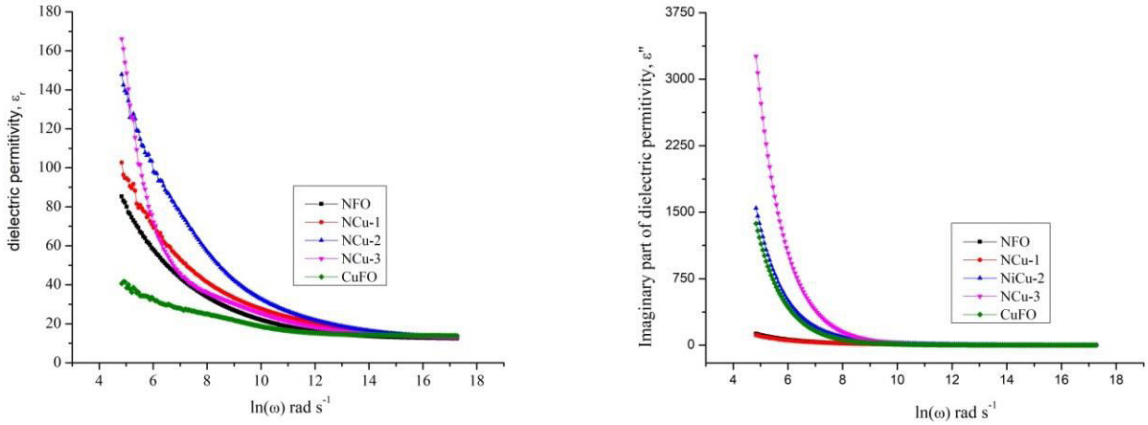

Fig.3 Variation of (a). Real Part of Dielectric constant, ε' with ln(ω) and (b) Imaginary Part of Dielectric constant, ε'' with ln(ω).

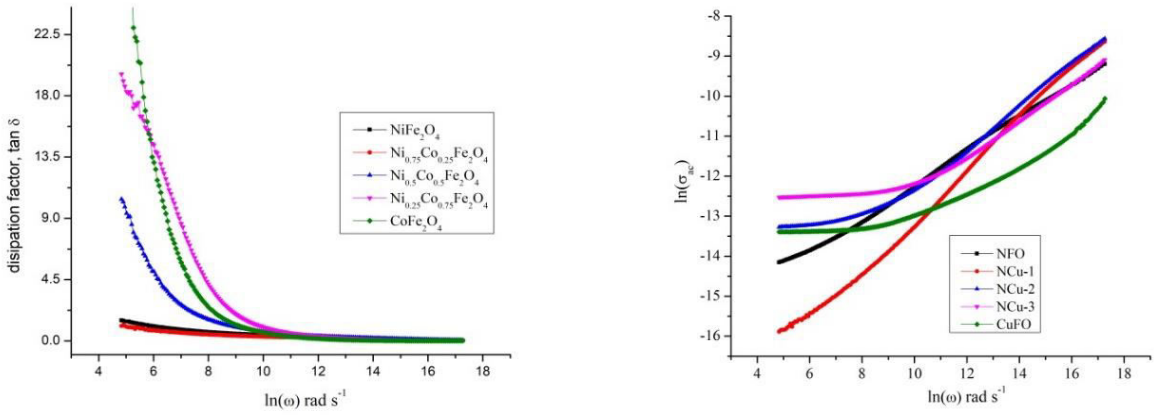

Fig.3 Variation of (c) Dissipation factor tanδ with ln(ω) and (d) AC conductivity, ln (σ_{ac}) with ln(ω).

3.3 Magnetic Studies

M-H loops at RT were recorded for all the proposed mixed ferrite-samples and are shown in Fig.4. From, M-H loops, it is clear that loops are saturated at higher field values, which is the characteristic feature of any ferri-magnetic material. It is observed that, the samples exhibited no hysteresis, very low coercivity which may be attributed to super paramagnetic nature of the samples [19-21]. Magnetic parameters such as M_S, M_r and Hc, were extracted from the obtained loops and measured parameters for all the samples are summarized in Table 1.

Table 1: Magnetic parameters obtained from M-H Loops.

Sample(s)	Saturation Magnetization **Ms** (emu/g)	Remanent Magnetization **Mr** (emu/g)	Coercive Field **Hc** (Oe)
$NiFe_2O_4$	34.79	3.41	75
$Ni_{0.75}Cu_{0.25}Fe_2O_4$	82.81	0.06	0.8
$Ni_{0.5}Cu_{0.5}Fe_2O_4$	53.33	3.56	20.25
$Ni_{0.25}Zn_{0.75}Fe_2O4$	42.95	11.75	122.58
$CuFe_2O4$	21.93	7.25	514.67

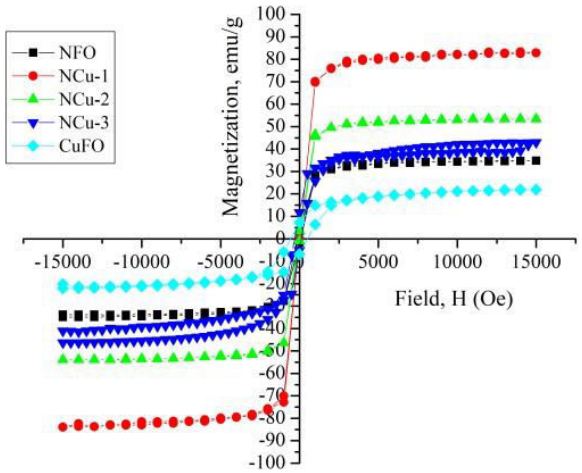

Fig.4 (a). Magnetic Hysteresis loops of $NiCuFe_2O_4$ mixed ferrite system

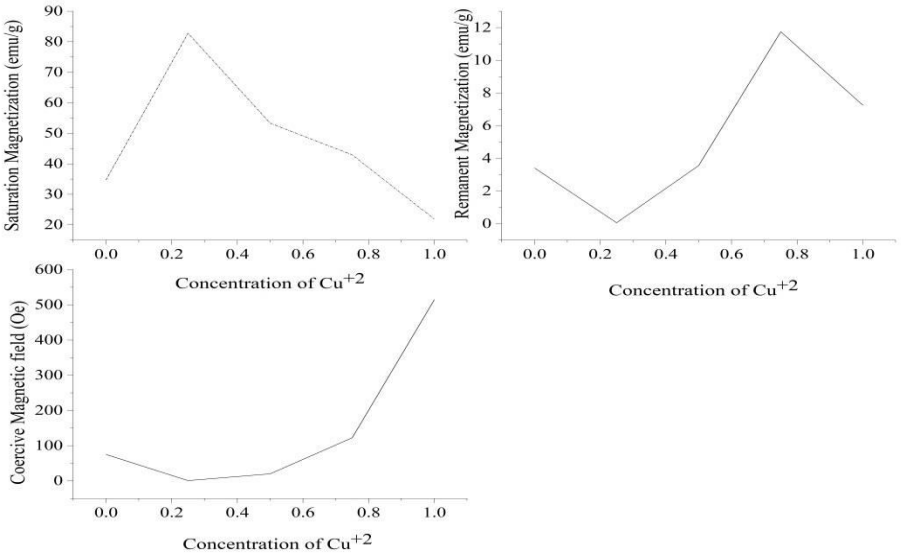

Fig.4 (b). Variation of magnetic parameters with Cu^{+2} concentration in NFO

CONCLUSIONS

Nano-powders of the system $Cu_xNi_{(1-x)}Fe_2O_4$ (here x=0, 0.25, 0.5, 0.75 and 1.0) were prepared successfully using wet-chemical method in which citric acid was used as an organic fuel so as to occur auto-combustion reaction which involves nitrate-citrate precursors. Structural phase is confirmed through PXRD studies for the proposed mixed $NiCuFe_2O_4$ system. Morphology of the nano-powders reveals the dense structures with well-defined grains. All the samples shown dielectric dispersion during their dielectric studies and as well as their ferromagnetic behavior is confirmed through magnetic measurements, in which the samples of mixed ferrite exhibited non-linear

nature when curves are drawn in between applied external magnetic field (H) and magnetization (M). These prepared mixed ferrite samples are having very minimal magnetic loss and very low coercive values, these characteristics of the proposed nano-powder samples are of technologically important and can be implemented in smart functional device applications.

ACKNOWLEDGEMENTS

Authors are highly thankful to CENSE, IISc-Bangalore for providing PXRD and FESEM facilities to accomplish this research work.

REFERENCES

1. D.Ravinder, Mater Letters, Vol.43, No.3, pp.129-138 (2000).
2. C Sujatha , K.V Reddy, K.S Babu, A.R Reddy, K.H Rao,Ceramic.Int, Vol.38, No 7, pp.5813-5820 (2012).
3. E.Ranjith Kumar, P.Siva Prasada Reddy, G Sarala Devi, S. Sathiyaraj, Jour.Magn.Magn.Mater, Vol.398, pp.281-288 (2016).
4. Valenzuela R, Phys. Res.Int, 2012 (2012).
5. J Liu, S Li, B. Zhang, Y. L Wang, Y.Gao, X.S Liang, Y.Wang, J.Colloid Intface.Sci,504, pp.206-213 (2017).
6. I.Kortidis, H.C Swart, S.S Ray, D.E Motaung, Sen.Actu B Chem, 285, pp.92-107 (2019).
7. M.Lakshmi, K.Vijaya kr, K.Thyagarajan , J.Nano.struct in Chem, 5(4), pp.365 (2015).
8. Abdallah H M I, Moyo T, Ngema N, Jour.Magn.Magn. Matr, 394, pp.223-228 (2015).
9. A.B Bodade, H.G Wankhade, G.N Chaudhari, D.C Kothari, Talanta, 89, pp.183 (2012).
10. S.Abdul Khader, Asiya Parveez, Arka Chaudhuri, M S Shekhawat and T.Sankarappa, Physica B: Condensed Matter, 584, May Issue, pp.411675 (2020).
11. Ahamad I, Ayesh, Mohammad Abu Hajija, Adeel Shaheen, Fawji Banat, Appl.Phy A 123,pp.682 (2017).
12. M.H Abdellatif, Claudia I, I Liakos, Alice S, S Marras, Marco S, Jour Magn.Magn.Matt 424, pp.402-409 (2017).
13. Mohammad Abu Hajija, Ayah F.S, Abu-Hani, Najwa Hamdan, S Stephen, Ahamad I, Ayesh, Jour.Alloys and Compounds 692, pp.461-468 (2017).
14. V.A Zhuravlev, R.V .Minin, V.I Itin, Yu Lilneko, Jour.Alloys& Comp 692 ,pp.705 (2017).
15. Wagner KW (1913) Ann Phys 40:817.
16. Maxwell JC, Electricity & Magnetism, Vol 1, Oxford Univ Press, Oxford (1929).
17. Koops CG (1951) Phys Rev 83:121.
18. J.Smitet H.P, J Wijn, Les.Ferrites, Dunod, Paris (1961).
19. P.Singh, D.Rathore, Jour. Appl. Phys, 1728, pp.20259 (2016).
20. Chikazumi S, Physics of Ferromagnetism, Oxford University Press, Oxford (1997).
21. E.C Stoner and E.P Wohlfarth. Phil. Trans. Roy. Soc.A 240, 599 (1948).